

Near IR to Red Up-Conversion in Tetracene/Pentacene Host/Guest Cocrystals Enhanced by Energy Transfer from Host to Guest

Teresa Gatti,^{†,‡} Luigi Brambilla,[†] Matteo Tommasini,[†] Francesca Villafiorita-Monteleone,[‡] Chiara Botta,[‡] Valerio Sarritzu,[§] Andrea Mura,[§] Giovanni Bongiovanni,[§] and Mirella Del Zoppo^{*,†}

[†]Politecnico di Milano Dipartimento di Chimica, Materiali e Ing. Chimica “G. Natta”, p.zza Leonardo da Vinci 32, 20133 Milano, Italy

[‡]Istituto per lo Studio delle Macromolecole, CNR, Via Bassini 15, I-20133 Milano, Italy

[§]Dipartimento di Fisica, Università di Cagliari, SLACS-INFM/CNR, I-09042 Monserrato (Cagliari), Italy

Received: February 26, 2015

Revised: July 6, 2015

Published: July 16, 2015

INTRODUCTION

Up-conversion (UC) at low power intensities is a very appealing phenomenon, which opens the way to many possible applications including solar harvesting, bioimaging, optical data storage, and many others. Triplet–triplet annihilation (TTA) UC has been demonstrated in several systems that comprise a liquid solution of triplet sensitizers and emitters.¹ More recently, this phenomenon has been realized also in solid polymer matrices, which are more suitable for potential applications.^{2–5} In this frame, the existence of other solid-state UC systems with no need of sensitizers may be of extreme interest, and in this work we show that acene host–guest crystalline systems can be successfully used for the purpose of converting near IR photons into visible (yellow-red) light. The rationale behind this choice relies on the following observations.

On one side, host–guest systems based on organic molecular crystals have recently provided a good platform for the design of functional materials with enhanced optoelectronic properties such as resonant energy transfer (RET),^{6–8} tunable fluorescence,⁹ and amplified spontaneous emission (ASE).¹⁰ Indeed, their structures offer a model to investigate relationships between molecular packing modes and optoelectronic features.

On the other side, acene-based dyes are known to have a significant fluorescence quantum yield in solution.¹¹ This efficiency is partly quenched when going to the solid state because of aggregation effects. Conversely, in order to obtain performing optoelectronic devices it is necessary to retain good

fluorescence efficiency also in the solid state. Recently, organic molecular host/guest cocrystals based on oligoacene materials have been shown to promote a very efficient host-to-guest energy transfer at very low concentrations of guest species.⁷ These can be thought of as substitutional defects and behave as isolated molecules in the surrounding environment of the host crystalline matrix. The large Förster-type resonant energy transfer (FRET)¹¹ shown by these systems has allowed us to obtain highly fluorescent polymer films which can be deposited on appropriate substrates using conventional wet processing techniques. In addition to retaining significant luminescence efficiency, these systems also offer the possibility of tailoring the converted emitted wavelength by changing the host/guest pair. This makes them suitable candidates as active components, e.g., in organic luminescent solar concentrators (OLSCs), which currently represent a promising technology to reduce manufacturing and installation costs of conventional photovoltaic modules.^{12–14} The preparation of fluorescent films based on poly(methyl methacrylate) (PMMA) doped with anthracene/tetracene (Ac/Tc) host/guest cocrystals was recently reported, together with their use as OLSCs for Si solar cells.¹⁵

In the present work we focus on the tetracene/pentacene host–guest crystalline system (Tc/Pc, Figure 1). This choice has the advantage of a longer emission wavelength with respect

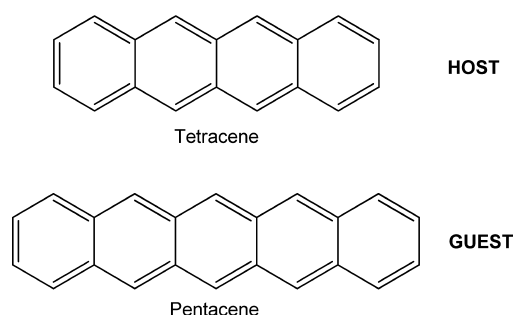


Figure 1. Molecular structures of the cocystal constituents: tetracene (host) and pentacene (guest).

to what was previously obtained with the use of the Ac/Tc couple;¹⁵ moreover, as reported below, the peculiar electronic structure of host and guest molecules makes it possible to combine efficient energy transfer to efficient TT recombination giving rise to UC.

Up to now cocrystalline host/guest systems of this type have been investigated for their potential use as down-converters of high-energy photons or light emission amplifiers. To the best of our knowledge, they have never been studied to up-convert (UC) low-energy photons,^{16,17} such as those in the NIR region, into visible photons.

EXPERIMENTAL SECTION

Cocrystal Synthesis. All chemicals and solvents were purchased from Sigma-Aldrich and used as received. A general procedure was employed for the preparation of tetracene/pentacene (Tc/Pc) cocrystals (here reported for the 50:1 molar ratio case). Tc (250 mg, 1.09 mmol) and Pc (6 mg, 0.021 mmol) were placed in a two-necked round-bottomed flask equipped with a condenser and kept under a gentle argon flux. Toluene (150 mL) was added, and the resulting orange suspension was stirred at room temperature for 5 min, ensuring protection from external light with an aluminum foil. Heating was turned on and continued until reflux temperature was reached. At this point more toluene was added, until complete dissolution of the remaining suspended solids was achieved (20 mL). The resulting solution was left standing and allowed to cool to room temperature slowly. Needle-shaped orange crystals formed which were filtered and dried in a vacuum oven at 70 °C for 30 min (247 mg).

Further recrystallization of the solution-derived material was carried out by sublimation diffusion using a homemade apparatus. The cocrystalline material (~5 mg) was inserted at the bottom of a glass tube, which was subsequently degassed under vacuum, refilled with Ar, and sealed, to ensure complete isolation from the external environment. The sealed tube was then placed in a heating chamber, leaving the upper part outside the heating zone. By allowing current to pass through the resistance surrounding the chamber, a temperature of approximately 220 °C was reached inside, as verified with a temperature sensor. Platelets like cocrystals grew inside the tube in the area immediately outside the heating chamber. After complete recrystallization the tube was removed from the chamber, allowed to cool to room temperature, and opened to extract the recrystallized material.

The anthracene/pentacene (Ac/Pc) cocrystalline material was prepared according to the following procedure (50:1 molar ratio): Ac (62 mg, 0.35 mmol) and Pc (2 mg, 0.007 mmol) were placed in a two-necked round-bottomed flask equipped

with a condenser and kept under a gentle argon flux. Chloroform (100 mL) was added, and stirring of the resulting suspension was carried out for 5 min at repair from light. The mixture was heated to reflux, whereupon all solids dissolved. At this point, condenser was removed while keeping the heating on, in order to completely evaporate chloroform. White Ac/Pc cocrystalline material formed at the bottom of the flask, which was allowed to cool to room temperature and dried *in vacuo* (64 mg).

Photoluminescence Spectroscopy. Photoluminescence (PL) spectra of solid-state materials were recorded on a Jasco Fp 6600 spectrofluorometer. The PL quantum yields (QY) were obtained using a homemade integration sphere following the procedure already reported.¹⁸

Power-dependent photoluminescence spectra of micrometric regions in the Tc/Pc cocrystals were recorded by using a Dilor Labram HR800 Raman spectrometer coupled with a BX41 Olympus microscope and a thermoelectrically cooled CCD detector. An Ar⁺ laser (line at 457 nm) and a solid-state laser (line at 785 nm) have been used as excitation sources. The exciting laser beam was focused on the samples with 20X or 50X Olympus objectives. Spectra are the average of four measurements with 0.5 or 1 s integration time, according to the maximum signal intensity to avoid detector saturation. The power density at the sample for the 457 nm laser was varied ranging from 9.3×10^3 to 4.1×10^6 mW cm⁻². The power density for the 785 nm laser was varied from 1.2×10^7 to 1.1×10^9 mW cm⁻². Photoluminescence spectra of different micrometric regions of recrystallized Tc under 785 nm excitation were recorded by varying the laser power from 1.2×10^7 up to 3.7×10^8 mW cm⁻². Photoluminescence spectra of different micrometric regions of Ac/Pc cocrystalline material under 785 nm excitation were recorded by varying laser power from 1.4×10^7 mW cm⁻² up to 1.1×10^9 mW cm⁻².

Time-Resolved Measurements. Time-resolved measurements were performed by using a mode locked Titanium:sapphire laser system operating at 80 MHz and delivering 100 fs long pulses (fwhm) with a cw mean power of about 500 mW at 780 nm. Optical excitation around 3.2 eV was obtained using a lithium iodate (LiIO₃) crystal as a frequency doubler. Laser pulses were focused down to a 80 μm spot on the samples, and the excitation power density was about 22 mW/cm². Photoluminescence was spectrally dispersed in a single spectrometer and temporally resolved with a visible 2D-streak camera (Hamamatsu C5680). The temporal resolution in the configuration we employed was of the order of 10 ps. Decay traces were extracted from streak camera spectrograms by integrating over a ~50 nm wide spectral window, while spectra at different delays were integrated over a ~100 ps wide temporal window. Up-conversion measurements were performed by using the same titanium:sapphire laser system both in the cw and pulsed regime. The excitation wavelength was at 780 nm with the same mean power in the two configurations. Laser light was focused down to a 15 μm spot, and the excitation power density was about 0.3 mW/μm². The collected signals were recorded with a LN-cooled CCD camera (Princeton Instruments 7439-0001) coupled to a grating spectrometer (Acton SP2500i).

RESULTS AND DISCUSSION

Synthesis and Photoluminescence Properties. Doped crystals were grown from hot toluene solutions. In this way needle-shaped crystals a hundred micrometers long have been

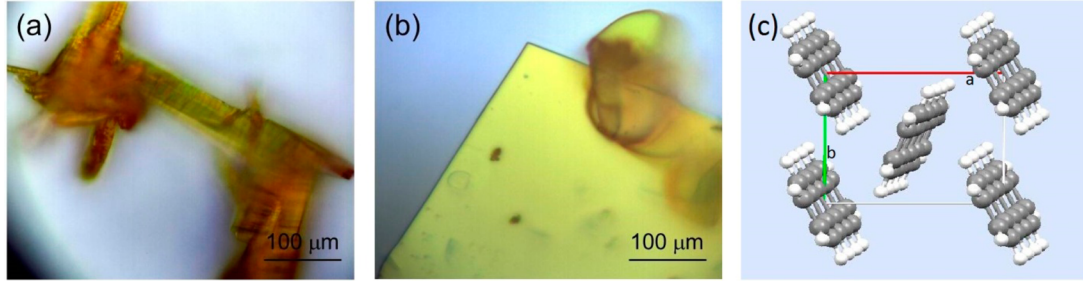


Figure 2. Microscope images of Tc/Pc cococrystalline materials. (a) Cococrystals resulting from solution crystallization. (b) Cococrystals obtained from recrystallization of solution-derived cococrystals. (c) Graphical representation of the molecular packing of Tc in the *ab* plane.

obtained (Figure 2a). Further recrystallization was achieved by sublimation diffusion of the crystalline material obtained from solution, resulting in a sample with platelet-like crystals with a size in the millimeter range and preferential growth along the *ab* plane of Tc (Figure 2b and 2c).

Samples with two different Tc:Pc molar ratios were investigated, namely, 350:1 and 50:1, showing different FRET efficiencies (Figure 3) and minor dependences on the crystal preparation method (see SI Figure S1).

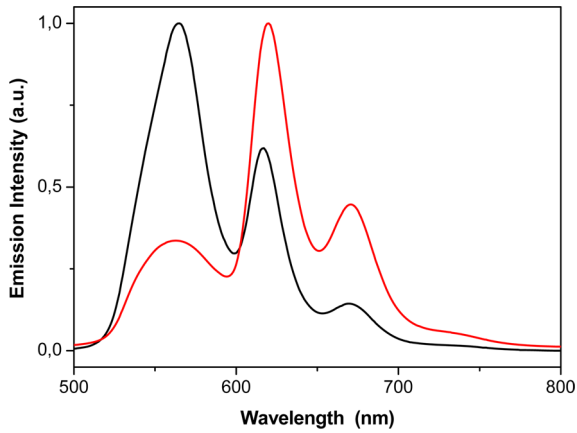


Figure 3. Photoluminescence spectra of Tc/Pc cococrystals obtained from toluene solution ($\lambda_{\text{exc}} = 400$ nm) with different molar ratios of the two components, respectively, 350:1 (black line) and 50:1 (red line).

The emission spectra of the cococrystals are characterized by three different peaks at 563, 616, and 670 nm, respectively. The higher energy peak is due to crystalline tetracene, and the two lower energy peaks are due to the 0–0 and 0–1 vibronic features of isolated pentacene, appearing at a longer wavelength with respect to the PL spectrum of the molecule in the gas phase¹⁹ and in solution,²⁰ as a result of the different surrounding environment.

The photoluminescence quantum yield (PLQY) excited at 400 nm, of the 50:1 (mol:mol) Tc/Pc cococrystal, has been measured and resulted to be 12% for the solution-derived material and 10% for the recrystallized material. Within the experimental uncertainty, the two PLQYs are to be considered the same value. In the more dilute cococrystal (350:1) the PLQY drops to 4%. These values are significantly higher with respect to pure crystalline Tc, for which a PLQY lower than 1% was estimated by us, in accordance with literature data.²¹ A possible explanation for the observed increase of PLQY in the Tc crystal upon Pc doping could be the partial disruption of the crystal

long-range order caused by the Pc guest molecules and the consequent reduction of exciton mobility toward nonradiative decay channels.¹⁰

The theoretical Förster radius (R_0) of the energy transfer from Tc to Pc of this system can be estimated with the formula²²

$$R_0^6 = 8.97 \times 10^{-5} [k^2 n^{-4} QY_D J] \quad (1)$$

where k^2 is the orientation factor, assumed to be 4 in the cococrystal;⁷ n is the refractive index of the medium (assumed to be 1.54 in Tc); QY_D is the PLQY of the host/donor in the absence of the guest/acceptor (assumed to be 0.008); and J expresses the degree of spectral overlap between the donor (Tc) emission and the acceptor (Pc) absorbance. The latter can be calculated as follows

$$J = \frac{\int_0^\infty F_D(\lambda) \epsilon_A(\lambda) \lambda^4 d\lambda}{\int_0^\infty F_D(\lambda) d\lambda} \cong 7.7 \times 10^{14} \text{ cm}^{-1} \text{ M}^{-1} \text{ nm}^4 \quad (2)$$

where F_D is the fluorescence spectrum of the donor and ϵ_A is the molar extinction coefficient of the acceptor (assumed to be $9900 \text{ cm}^{-1} \text{ M}^{-1}$ at the absorption maximum).²³ The value of R_0 resulting from the use of eqs 1 and 2 is 2.7 nm, a suitable distance for efficient FRET to take place.

Different regions of the cococrystals were investigated focusing a 457 nm laser beam, under a microscope objective, on $0.86 \mu\text{m}^2$ areas evidencing the presence of some inhomogeneities in the microscopic Tc/Pc relative concentrations. The inhomogeneity of the sample reduces the FRET efficiency due to the presence of crystal regions where Pc concentration is lower than the nominal one. As a consequence, the experimental FRET efficiency results are lower than the theoretical one (see SI). For a fixed sampled area, all the spectra presented a similar dependence of the emission intensity vs incident laser power, namely, a linear relationship when considering Tc emission and a slower growth law with a saturation regime for Pc emission (see SI Figures S3 and S4). The linear behavior likely indicates that emission from the first excited singlet of Tc (Tc-S1) takes place immediately after light excitation, whereas emission from Pc takes place mostly from Pc-S1 states populated through energy transfer from Tc-S1. This behavior can be explained taking into account the fact that Pc emission is comprised of two contributions: direct excitation with the consequent emission from Pc-S1 states (which gives a linear dependency on laser power as observed for Tc) and the excitation mediated by the energy-transfer (host–guest) processes which are governed by the k_{ET} rate constant ($dn/dt = k_{\text{ET}}[N]$) and which therefore saturate at high laser excitation powers. Due to

the small number of dopant molecules in the cocrystal, the first kind of contribution should be smaller.

Changing the excitation laser line from 457 to 785 nm to record a Raman spectrum free from the fluorescence background of Tc, one would not expect to observe any emission in the anti-Stokes region. On the contrary, as reported in Figure 4,

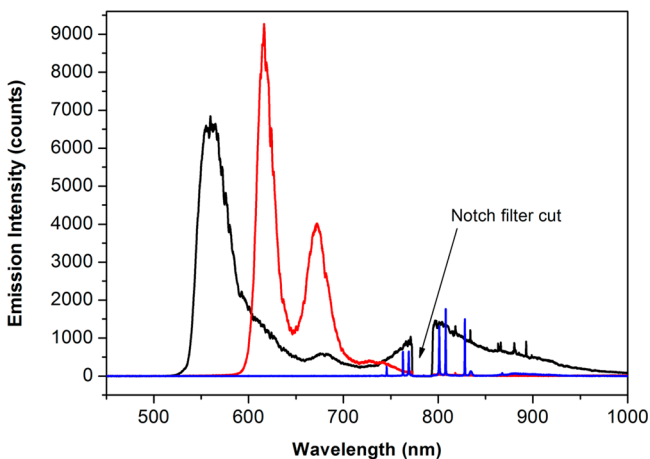


Figure 4. Stokes and anti-Stokes region of the Raman spectra of recrystallized Tc (black line), recrystallized Pc -doped Tc (red line) under 785 nm laser excitation with 1.4×10^8 mW cm⁻² power density, and recrystallized Pc (blue line) under 785 nm laser excitation with 1.1×10^9 mW cm⁻² power density.

the cocrystal shows the characteristic emission of isolated Pc at 616 and 670 nm, with no signal from host Tc. Probing different regions of the sample one obtains similar results.

The same experiment carried out on pure crystalline Tc (785 nm excitation) shows that also in this case there is an up-converted emission at 560 nm. This proves that (i) up-converted emission is possible in Tc and (ii) in the Tc–Pc cocrystal, up-conversion is attained, but the emitting species, in spite of its lower concentration, is Pc.

We notice that up-converted emission from Pc is obtained at laser power densities of the order of 1×10^7 mW/cm², and its intensity grows with the square of the incident laser power in all the different areas of the samples probed (see SI Figure S6). This indicates that this is a two-photon -initiated process which

involves excitation of two molecular species, energy transport in the crystal and bimolecular recombination. Similar results are found also in the case of pure Tc (see SI Figure S8).

The role of the Tc matrix on the up-conversion mechanism is demonstrated when considering that the excitation with 785 nm light of pure Pc and Ac/Pc cocrystals (prepared with a molar ratio similar to that used for Pc/Tc) does not yield any up-converted emission unless we reach high enough laser powers (1.1×10^9 mW/cm²). Under such an excitation condition, we started observing in the former case the Raman signals of Pc and in the latter very weak fluorescence signals from both Ac and Pc in addition to Ac Raman signals (see SI Figure S9). The appearance of the Raman signal, which is orders of magnitude weaker than fluorescence emission, further confirms the lack of up-converted Pc emission.

Time-Resolved Photoluminescence. The energy transfer dynamics is analyzed by time-resolved measurements (see Figure 5). At short delay times (less than 100 ps) the PL spectrum of the cocrystal shows mainly the Tc emission at 560 nm, while at longer times the growth of the peaks at 616 and 670 nm is assigned to pentacene emission. As shown in the inset of Figure 5a the Tc decay time observed in pure Tc crystal is longer (220 ps) than in the cocrystal (90 ps). The quenching of the Tc emission observed in the cocrystal is a consequence of the energy transfer to the Pc molecules, as proven by the rise of the Pc emission observed in the first 200 ps (see inset of Figure 5b).

Up-Conversion Mechanism. To the best of our knowledge up-converted emission from Tc without the presence of suitable sensitizers has never been observed before. In order to explain the mechanism generating this laser-induced UC process, we can try to formulate a reasonable hypothesis by considering what is widely recognized on the behavior of excited states in Tc crystals. Singlet fission (SF) in Tc has been observed and thoroughly studied.^{24–26} Triplet–triplet annihilation (TTA, the reverse process of SF) takes place when two triplets encounter and generate one molecule in an excited singlet state and another one in the ground state. This process is thermodynamically allowed in solid Tc (since $E(S_1) \leq 2E(T_1)$) but not in Pc.²⁵ The up-converted emission in pure Tc crystals and in Pc-doped Tc crystals might therefore originate from TTA, which is an intrinsically bimolecular process and

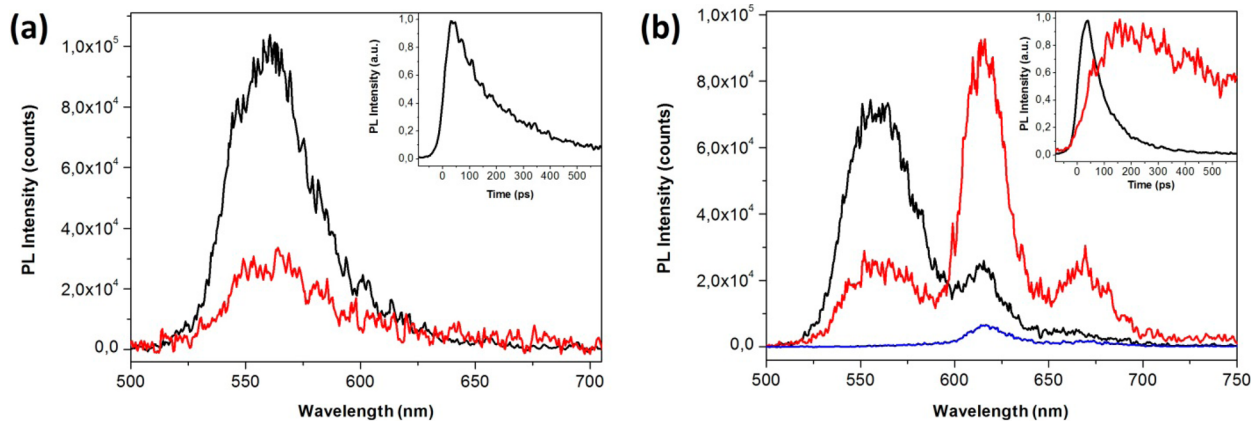


Figure 5. (a) PL spectra of Tc crystal recorded at different delay times: 70 ps (black line) and 1200 ps (red line). In the inset the decay dynamics of Tc emission at 560 nm. (b) PL spectra of Tc:Pc cocrystal 50:1 recorded at different delay times: 40 ps (black line), 215 ps (red line), and 1600 ps (blue line). In the inset the decay dynamics of Tc emission at 560 nm and Pc emission at 670 nm.

accounts for the quadratic trend found in the relationship between emission intensity vs incident laser power.

A possible alternative explanation for the observed Tc emission could be the direct excitation of singlet excitons via a simultaneous absorption of two photons. To this aim, we compared the Tc emission excited by a train of 100 fs long pulses and a cw laser, both having the same NIR photon energy and average intensity. However, the peak power of the pulsed excitation, being much higher than the one of the cw laser, should lead to a much more intense emission in the visible. At odds with this hypothesis, pulsed and cw excitation gave similar emission intensities. Accordingly, we rule out a direct two-photon absorption process as a possible explanation of Tc emission when excited by cw NIR light excitation.

Figure 6 reports the spectrogram of the PL emission excited by an 80 MHz train of 100 fs long laser pulses peaked at 785

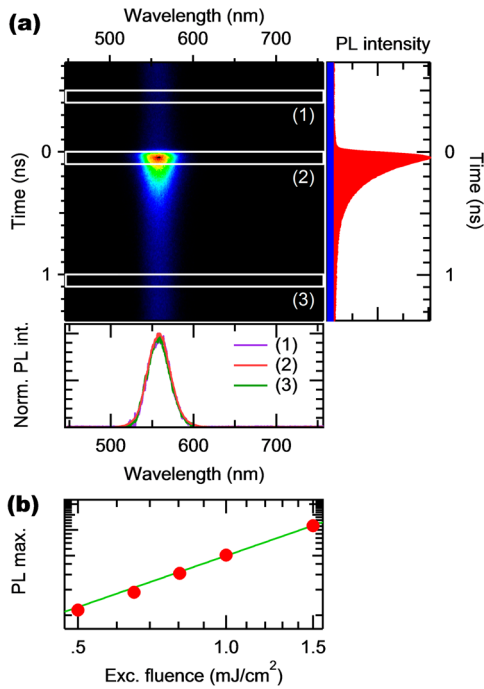


Figure 6. (a) Spectrogram (spectrum as a function of time) of the Tc PL emission excited by 100 fs long laser pulses with a fluence of 1 mJ/cm² at 785 nm. The spectrogram is reported as a false-color two-dimensional image. The right panel reports the temporal evolution of the spectral integrated signal. The red area highlights the transient PL signal, while the blue area highlights the long-lived contribution. The lower inset shows the spectrum of the PL signal integrated over a 100 ps time window: for negative delay (violet spectrum, region 1), zero delay (green spectrum, region 2), and positive delay (orange spectrum, region 3). (b) Maximum intensity of the PL spectrogram as a function of the excitation pulse fluence. The green line represents a quadratic fit to the experimental data.

nm. The Tc emission shows a transient contribution, highlighted by the red area in the right inset of Figure 6, on top of a long-lived emission (blue area). This latter contribution has a lifetime much longer than the time separation (12 ns) between laser pulses, as demonstrated by the detection of the Tc emission at negative times, i.e., before the arrival of the n th laser pulse and due to the pile-up of the emission excited by all the previous pulses. The spectra of the transient and long-lived contributions are identical, as shown in the lower inset of panel a, and their relative intensity is

independent of the excitation pulse fluence. The Tc emission scales quadratically with the laser intensity (Figure 6, panel b). The ratio between the quantum yield of the transient and long-lived PL emissions can be easily calculated from the spectrogram and results to be around 0.5 (the intensity of the long-lived PL signal is assumed nearly constant between pulses). The observation of the transient emission can be explained assuming a direct excitation of singlet excitons via the simultaneous absorption of two photons. The long-lived emission is consistent with the hypothesis of an indirect generation of long-lived population of triplets. Triplets decay via a TTA process to singlet excitons, which eventually undergo a fast radiative decay. We finally note that the simultaneous absorption of two photons is possible only under pulsed excitation, while it is certainly negligible under cw-optical pumping.

The main issue related to this explanation lies in the feasibility of direct triplet excitation by means of laser light in the host material. More likely, light excitation (for instance in the form of an inelastic light scattering process) causes the population of some “intermediate” state, which can sub-sequently de-excite and populate triplet states. Triplet excitons thus generated can then diffuse through the crystal lattice and recombine at trapping or defect sites located in the crystal. When considering pure Tc crystals, TTA populates Tc excited singlets, which then radiatively decay through fluorescence (Figure 7a).²⁷

On the other hand, when considering Pc-doped Tc crystals, the TT recombination sites might be associated in great majority to the Pc substitutional defects in the Tc crystal lattice. As a consequence, TTA of two Tc triplets takes place mainly at the Pc sites, which are present in the crystal in a larger number with respect to other types of defects or traps and are more homogeneously distributed in the sample. This causes the population of Pc excited singlet state, which then radiatively decays (Figure 7b).

As to the nature of this “intermediate” state, further investigation is needed. For the time being our data show that there exist some broad and featureless emission at around 800 nm which could be associated with this state and which has been observed in many polycondensated aromatic compounds (e.g., acenes, acene derivatives, perylene systems, etc.). Whether this state is involved in the population mechanism of triplet states is being investigated together with the assessment of its origin. At present we cannot draw any final conclusion; however, an indication that this state is associated with the aggregation state of the sample comes from the pressure-dependent behavior shown in Figure 8. In this figure we report the Raman spectra obtained in a diamond cell before applying the pressure, during pressure application, and after pressure removal.²⁸ As can be seen, when pressure is applied on the material, the up-converted emission red-shifts and decreases in intensity, to come back at similar position and intensity after pressure removal. Under pressure the emission at 800 nm is enhanced indicating that either (i) the increased intermolecular interactions favor the population and hence the emission from this state or (ii) since under pressure the up-conversion efficiency decreases, probably because of hindered excitation diffusion, the population of the excited intermediate state is relaxed via direct emission. This second hypothesis supports the existence of a relationship between the population of the intermediate state and the excitation of the triplet states involved in TTA mechanism.

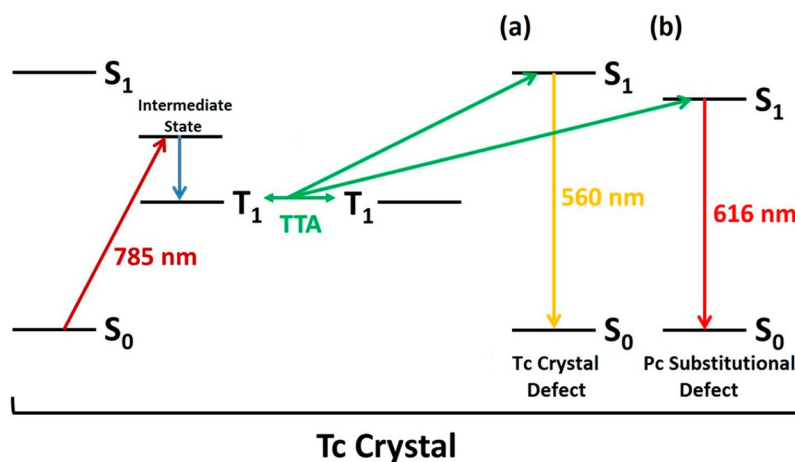


Figure 7. Schematic representation of the mechanism proposed to rationalize UC emission under 785 nm laser excitation at 560 nm in pure Tc crystal (a) and at 616 nm in Pc-doped Tc crystal (b).

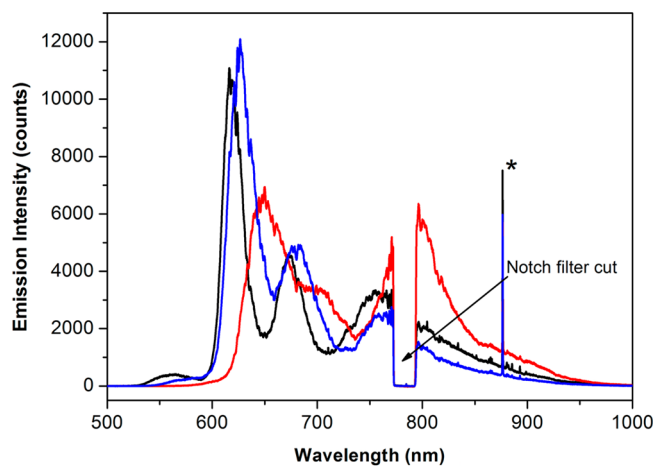


Figure 8. Up-converted emission spectra of 350:1 tetracene/pentacene cocrystals in a diamond cell ($\lambda_{\text{exc}} = 785 \text{ nm}$) before applying a pressure (black line), during pressure application (red line), and after pressure removal (blue line) obtained at $9.7 \times 10^7 \text{ mW cm}^{-2}$ laser power density. (Asterisk indicates diamond Raman band which can be used as an internal standard.)

Finally, measurements done on Tc in solution (see SI Figure S12) show that UC in Tc isolated molecules does not occur, thus supporting the idea that energy transfer from Tc to Pc is involved in the UC emission of the guest species in the cocrystals.

Quantum Chemical Calculations. Quantum chemical B3LYP/6-31G(d,p) TDDFT²⁹ calculations have been carried out on selected molecular models to provide some further support to the experimental findings. To this purpose we carried out quantum chemical calculations on model cluster systems composed by assemblies of Tc and Pc molecules (see SI for details). From these calculations we deduce that a sizable exciton coupling exists not only in the case of pure Tc but also for Pc embedded in Tc. The existence of a strong exciton coupling occurring in the solid state^{30,1-5} is the physical basis for good exciton transport and diffusion across Tc/Pc molecular crystals, one of the key elements of the mechanism proposed in Figure 7.

CONCLUSIONS

In conclusion, we presented a cocrystalline system based on oligoacene compounds, in which Tc was used as the host matrix and Pc as the guest dopant. FRET from Tc to Pc guest, characterized by a theoretical Förster radius of about 23 Å, takes place efficiently only at rather high dopant concentrations (50:1). Pc doping appears to favor the radiative deactivation of the Tc excited state, the PLQY being an order of magnitude larger than that of pure crystalline Tc.

Apparently, even more efficient FRET originates in the system when NIR light excitation is employed, giving rise to UC emission. Indeed, when exciting with 785 nm laser light, only the emission from Pc (guest) is observed, with no trace of Tc (host) emission. This phenomenon is due to the occurrence of a radiative delayed bimolecular exciton recombination in the system, as shown also by time-resolved measurements. Recombination of the photogenerated species preferentially occurs at defect sites, mainly represented by isolated Pc molecules in the Tc crystal lattice. Our future efforts will be therefore addressed toward unraveling the exact mechanism underlying this process, together with the evaluation of its quantum efficiency. At present we want to underline the broad relevance of the observations presented in this work, which might allow us to stimulate further research addressed at finding more efficient up-converting systems based on all-organic cocrystalline systems, thus avoiding the use of heavy metal components, which are commonly employed as triplet sensitizers for TTA-promoted UC applications.

ASSOCIATED CONTENT

Supporting Information

The Supporting Information is available free of charge on the ACS Publications website.

PL spectra of recrystallized Tc/Pc ($\lambda_{\text{exc}} = 457, 785 \text{ nm}$) with different excitation intensities; theoretical and experimental energy transfer efficiency; PL spectra of Tc and Ac/Pc crystals ($\lambda_{\text{exc}} = 785 \text{ nm}$) with different excitation intensities; optical microscope images of Tc and Ac/Tc crystals; PL spectrum of Tc in CHCl_3 solution ($\lambda_{\text{exc}} = 785 \text{ nm}$). Quantum chemical calculations on model systems (PDF)

AUTHOR INFORMATION

Corresponding Author

*E-mail: mirella.delzoppo@polimi.it.

Present Address

¹Università di Padova Dipartimento di Scienze Chimiche, via Marzolo 1, 35131 Padova, Italy.

Author Contributions

The manuscript was written through contributions of all authors. All authors have given approval to the final version of the manuscript.

Notes

The authors declare no competing financial interest.

ABBREVIATIONS

Tc, tetracene; Pc, pentacene; Ac, anthracene; UC, up-conversion; TTA, triplet triplet annihilation; PL, photoluminescence; PLQY, photoluminescence quantum yield; FRET, fluorescence resonance energy transfer; TDDFT, time dependent density functional theory

REFERENCES

(1) Zhao, J.; Ji, S.; Guo, H. Triplet–triplet Annihilation Based Upconversion: From Triplet Sensitizers and Triplet Acceptors to Upconversion Quantum Yields. *RSC Adv.* **2011**, *1*, 937.

(2) Islangulov, R. R.; Lott, J.; Weder, C.; Castellano, F. N. Noncoherent Low-Power Upconversion in Solid Polymer Films. *J. Am. Chem. Soc.* **2007**, *129*, 12652–12653.

(3) Simon, Y. C.; Weder, C. Low-Power Photon Upconversion through Triplet–triplet Annihilation in Polymers. *J. Mater. Chem.* **2012**, *22*, 20817.

(4) Monguzzi, A.; Mezyk, J.; Scotognella, F.; Tubino, R.; Meinardi, F. Upconversion-Induced Fluorescence in Multicomponent Systems: Steady-State Excitation Power Threshold. *Phys. Rev. B: Condens. Matter Mater. Phys.* **2008**, *78*, 195112.

(5) Monguzzi, A.; Tubino, R.; Hoseinkhani, S.; Campione, M.; Meinardi, F. Low Power, Non-Coherent Sensitized Photon up-conversion: Modelling and Perspectives. *Phys. Chem. Chem. Phys.* **2012**, *14*, 4322–4332.

(6) Park, S. K.; Varghese, S.; Kim, J. H.; Yoon, S.-J.; Kwon, O. K.; An, B.-K.; Gierschner, J.; Park, S. Y. Tailor-Made Highly Luminescent and Ambipolar Transporting Organic Mixed Stacked Charge-Transfer Crystals: An Isometric Donor-Acceptor Approach. *J. Am. Chem. Soc.* **2013**, *135*, 4757–4764.

(7) Wang, H.; Yue, B.; Xie, Z.; Gao, B.; Xu, Y.; Liu, L.; Sun, H.; Ma, Y. Controlled Transition Dipole Alignment of Energy Donor and Energy Acceptor Molecules in Doped Organic Crystals, and the Effect on Intermolecular Förster Energy Transfer. *Phys. Chem. Chem. Phys.* **2013**, *15*, 3527–3534.

(8) Viani, L.; Tolbod, L. P.; Jazdzzyk, M.; Patrinoiu, G.; Cordella, F.; Mura, A.; Bongiovanni, G.; Botta, C.; Beljonne, D.; Hanack, M.; et al. Spatial Control of 3D Energy Transfer in Supramolecular Nanostructured Host - Guest Architectures. *J. Phys. Chem. B* **2009**, *113*, 10566–10570.

(9) Zhao, Y. S.; Fu, H. B.; Hu, F. Q.; Peng, a. D.; Yang, W. S.; Yao, J. N. Tunable Emission from Binary Organic One-Dimensional Nanomaterials: An Alternative Approach to White-Light Emission. *Adv. Mater.* **2008**, *20*, 79–83.

(10) Wang, H.; Li, F.; Gao, B.; Xie, Z.; Liu, S.; Wang, C.; Hu, D.; Shen, F.; Xu, Y.; Shang, H.; et al. Doped Organic Crystals with High Efficiency, Color-Tunable Emission toward Laser Application. *Cryst. Growth Des.* **2009**, *9*, 4945–4950.

(11) Valeur, B. *Molecular Fluorescence Principles and Applications*; Wiley-VCH: Weinheim, 2002.

(12) Beverina, L.; Sanguineti, A. Organic Fluorophores for Luminescent Solar Concentrators. In *Solar Cell Nanotechnology*;

Tiwari, A., Boukherroub, R., Sharon, M., Ed.; John Wiley & Sons: Hoboken, NJ, USA.

(13) Botta, C.; Betti, P.; Pasini, M. Organic Nanostructured Host–guest Materials for Luminescent Solar Concentrators. *J. Mater. Chem. A* **2013**, *1*, 510.

(14) Currie, M. J.; Mapel, J. K.; Heidel, T. D.; Goffri, S.; Baldo, M. A. High-Efficiency Organic Solar Concentrators for Photovoltaics. *Science (Washington, DC, U. S.)* **2008**, *321*, 226–228.

(15) Griffini, G.; Brambilla, L.; Levi, M.; Castiglioni, C.; Del Zoppo, M.; Turri, S. Anthracene/tetracene Cocrystals as Novel Fluorophores in Thin-Film Luminescent Solar Concentrators. *RSC Adv.* **2014**, *4*, 9893.

(16) De Wild, J.; Meijerink, a.; Rath, J. K.; van Sark, W. G. J. H. M.; Schropp, R. E. I. Upconverter Solar Cells: Materials and Applications. *Energy Environ. Sci.* **2011**, *4*, 4835.

(17) Gray, V.; Dzebo, D.; Abrahamsson, M.; Albinsson, B.; Moth-Poulsen, K. Triplet-Triplet Annihilation Photon-Upconversion: Towards Solar Energy Applications. *Phys. Chem. Chem. Phys.* **2014**, *16*, 10345–10352.

(18) Moreau, J.; Giovanella, U.; Bombenger, J. P.; Porzio, W.; Vohra, V.; Spadacini, L.; Di Silvestro, G.; Barba, L.; Arrighetti, G.; Destri, S.; et al. Highly Emissive Nanostructured Thin Films of Organic Host-Guests for Energy Conversion. *ChemPhysChem* **2009**, *10*, 647–653.

(19) Halasinski, T. M.; Hudgins, D. M.; Salama, F.; Allamandola, L. J.; Bally, T. Electronic Absorption Spectra of Neutral Pentacene (C₂₂H₁₄) and Its Positive and Negative Ions in Ne, Ar, and Kr Matrices. *J. Phys. Chem. A* **2000**, *104*, 7484–7491.

(20) Sakamoto, Y.; Suzuki, T.; Kobayashi, M.; Gao, Y.; Fukai, Y.; Inoue, Y.; Sato, F.; Tokito, S. Perfluoropentacene: High-Performance P-N Junctions and Complementary Circuits with Pentacene. *J. Am. Chem. Soc.* **2004**, *126*, 8138–8140.

(21) Bowen, E. J.; Mikiewicz, E.; Smith, F. W. Resonance Transfer of Electronic Energy in Organic Crystals. *Proc. Phys. Soc., London, Sect. A* **1949**, *62*, 26.

(22) Lakowicz, J. R. *Principles of Fluorescence Spectroscopy*; Kluwer Aca.: New York, 1999.

(23) Hellner, C.; Lindqvist, L.; Roberge, P. C. Absorption Spectrum and Decay Kinetics of Triplet Pentacene in Solution, Studied by Flash Photolysis. *J. Chem. Soc., Faraday Trans. 2* **1972**, *68*, 1928–1937.

(24) Smith, M. B.; Michl, J. Singlet Fission. *Chem. Rev.* **2010**, *110*, 6891–6936.

(25) Zimmerman, P. M.; Bell, F.; Casanova, D.; Head-Gordon, M. Mechanism for Singlet Fission in Pentacene and Tetracene: From Single Exciton to Two Triplets. *J. Am. Chem. Soc.* **2011**, *133*, 19944–19952.

(26) Wilson, M. W. B.; Rao, A.; Johnson, K.; Gelinias, S.; Pietro, R.; Clark, J.; Friend, R. H. Temperature-Independent Singlet Exciton Fission in Tetracene. *J. Am. Chem. Soc.* **2013**, *135*, 16680–16688.

(27) Burdett, J. J.; Müller, A. M.; Gosztoła, D.; Bardeen, C. J. Excited State Dynamics in Solid and Monomeric Tetracene: The Roles of Superradiance and Exciton Fission. *J. Chem. Phys.* **2010**, *133*, 144506.

(28) Even if a quantitative pressure determination has not been possible a reasonable estimate of the applied pressure is in the range of GPa.

(29) Frisch, M. J.; Trucks, G. W.; Schlegel, H. B.; Scuseria, G. E.; Robb, M. A.; Cheeseman, J. R.; Scalmani, G.; Barone, V.; Mennucci, B.; Petersson, G. A.; et al. *Gaussian 09*, revision A.02; Gaussian, Inc.: Wallingford, CT, 2009.

(30) Quarti, C.; Fazzi, D.; Del Zoppo, M. A Computational Investigation on Singlet and Triplet Exciton Couplings in Acene Molecular Crystals. *Phys. Chem. Chem. Phys.* **2011**, *13*, 18615–18625.